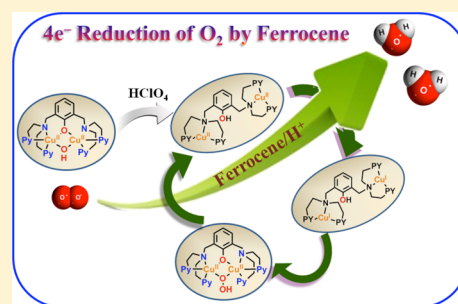


Acid-Induced Mechanism Change and Overpotential Decrease in Dioxygen Reduction Catalysis with a Dinuclear Copper Complex

Dipanwita Das,[†] Yong-Min Lee,[†] Kei Ohkubo,[§] Wonwoo Nam,^{*,†} Kenneth D. Karlin,^{*,†,‡} and Shunichi Fukuzumi^{*,†,§}[†]Department of Bioinspired Science, Ewha Womans University, Seoul 120-750, Korea[‡]Department of Chemistry, The Johns Hopkins University, Baltimore, Maryland 21218, United States[§]Department of Material and Life Science, Division of Advanced Science and Biotechnology, Graduate School of Engineering, Osaka University, Suita, Osaka 565-0871, Japan

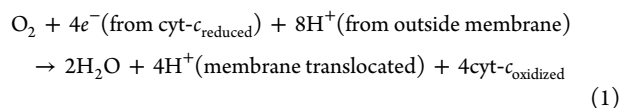
S Supporting Information

ABSTRACT: Catalytic four-electron reduction of O₂ by ferrocene (Fc) and 1,1'-dimethylferrocene (Me₂Fc) occurs efficiently with a dinuclear copper(II) complex [Cu^{II}₂(XYLO)(OH)]²⁺ (**1**), where XYLO is a *m*-xylene-linked bis[(2-(2-pyridyl)ethyl)amine] dinucleating ligand with copper-bridging phenolate moiety, in the presence of perchloric acid (HClO₄) in acetone at 298 K. The hydroxide and phenoxo group in [Cu^{II}₂(XYLO)(OH)]²⁺ (**1**) undergo protonation with HClO₄ to produce [Cu^{II}₂(XYLOH)]⁴⁺ (**2**) where the two copper centers become independent and the reduction potential shifts from −0.68 V vs SCE in the absence of HClO₄ to 0.47 V; this makes possible the use of relatively weak one-electron reductants such as Fc and Me₂Fc, significantly reducing the effective overpotential in the catalytic O₂-reduction reaction. The mechanism of the reaction has been clarified on the basis of kinetic studies on the overall catalytic reaction as well as each step in the catalytic cycle and also by low-temperature detection of intermediates. The O₂-binding to the fully reduced complex [Cu^I₂(XYLOH)]²⁺ (**3**) results in the reversible formation of the hydroperoxo complex ([Cu^{II}₂(XYLO)(OOH)]²⁺) (**4**), followed by proton-coupled electron-transfer (PCET) reduction to complete the overall O₂-to-2H₂O catalytic conversion.



INTRODUCTION

The heme/copper (heme *a*₃/Cu_B) heterodinuclear center in cytochrome *c* oxidases (CcO) catalyzes the four-electron and four-proton reduction of dioxygen (O₂) to water in the final stage of the respiratory chain (eq 1).^{1–4}



The catalytic four-electron reduction of O₂ to water has attracted much interest because of the important role in respiration⁵ and also potential application in fuel cell technology.⁶ The four-electron reduction of O₂ is catalyzed by platinum instilled in carbon at the cathode in fuel cells.^{6–9} To achieve substantial activity, high loadings of this precious metal are required which have prompted research efforts to develop catalysts based on nonprecious metals such as Co and Fe.^{10–18} Cu catalysts have also merited considerable interest,^{19–24} in relation with copper containing enzymes, the so-called multicopper oxidases (MCOs), which efficiently effect the four-electron four-proton reduction to water as part of their function.^{25–28}

In contrast to such heterogeneous systems, investigations on the catalytic reduction of O₂ by metal complexes in homogeneous systems have provided deeper insight into the

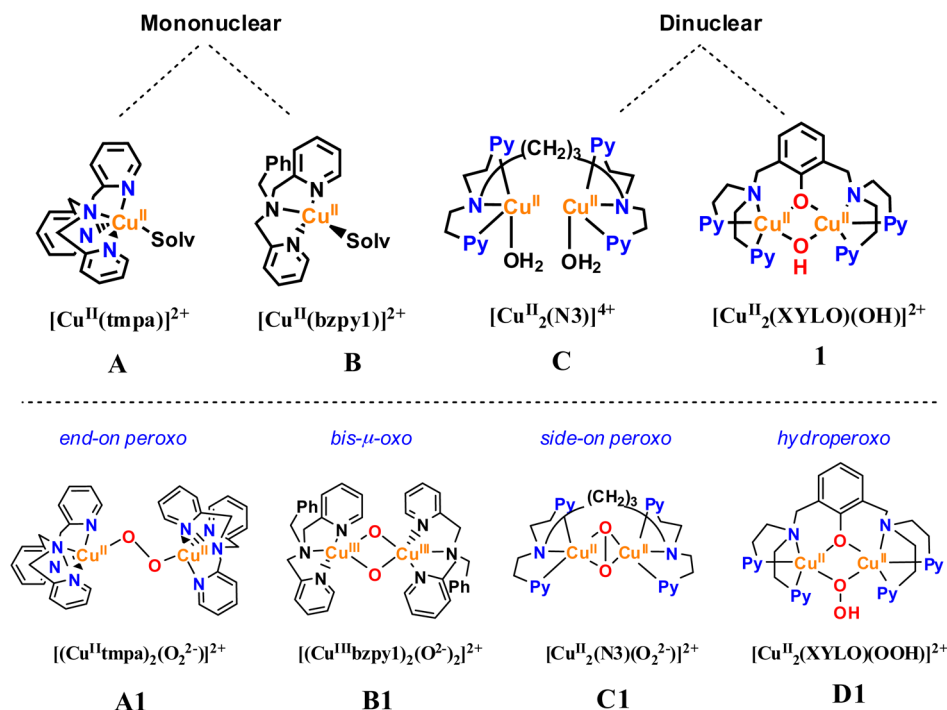
catalytic mechanism of the two-electron and four-electron reduction of O₂. Solution variable-temperature kinetic studies and detection of reactive metal–O₂ intermediates reveal the controlling factors in the two- vs four-electron reduction of O₂ with metal complexes.^{29–35} The key feature is the modification of supporting ligand environments which can allow for differing copper–dioxygen intermediates.

So far we found that two mononuclear copper complexes having tmpa (tmpa = tris(2-pyridylmethyl)amine) (**A**),³⁶ bzpy1 = *N,N*-bis[2-(2-pyridyl)ethyl]benzylamine (**B**)³⁷ and one dinuclear copper complex with N3 ligand (N3 = $-(\text{CH}_2)_3$ -linked bis[(2-(2-pyridyl)ethyl)amine])³⁷ (**C**) (Scheme 1) efficiently catalyze the four-electron reduction of dioxygen via the formation of [(tmpa)Cu^{II}]₂(μ-1,2-O₂²⁻)²⁺ (**A1**), [Cu^{III}]₂(bzpy1)(μ-(O²⁻)₂)²⁺ (**B1**) and [Cu^{II}]₂(N3)(μ-η²:η²-O₂²⁻)²⁺ (**C1**) intermediates, respectively, which were prone to proton-promoted reductive O–O cleavage to give water, in preference to simple protonation leading to H₂O₂.^{36,37} However, the dinuclear copper(II) complex [Cu^{II}₂(XYLO)(OH)]²⁺ (**1**) (Scheme 1), where XYLO is a *m*-xylene-linked bis[(2-(2-pyridyl)ethyl)amine] dinucleating ligand with copper-bridging phenolate moiety, catalyzes the two-electron reduction

Received: December 18, 2012

Published: February 26, 2013

Scheme 1



of O_2 to hydrogen peroxide in the presence of trifluoroacetic acid (HOTf) via the hydroperoxo intermediate (**D1**).³⁸ In all cases, however, only a strong one-electron reductant such as decamethylferrocene (Fc^*) could be used to reduce O_2 with the copper complexes. There has so far been no example for the catalytic reduction of O_2 by one-electron reductants weaker than Fc^* with Cu complexes.

We report herein that $[\text{Cu}^{\text{II}}_2(\text{XYLO})(\text{OH})]^{2+}$ (**1**) can instead act as an efficient catalyst for the four-electron reduction of O_2 by one-electron reductants weaker than Fc^* such as ferrocene (Fc) and 1,1'-dimethylferrocene (Me_2Fc) in the presence of HClO_4 in acetone. The reasons why the same catalyst can act in either the two-electron or four-electron reduction of O_2 by Fc^* and Fc in the presence of CF_3COOH and HClO_4 , respectively, are elucidated on the basis of new kinetic studies on the overall catalytic reactions as well as each catalytic step and also by detection of copper–dioxygen-derived intermediates which form during the catalytic cycle. The present study leads to successful achievement of two important features, which have never been previously observed:

- We have been able to effect catalytic O_2 reduction using significantly less overpotential with a dinuclear copper complex, which is of course more desirable and more energy efficient.
- We have been able to change the number of electrons in the catalytic reduction of O_2 from two electrons to four electrons by only increasing the acidity of the proton source employed.

The mechanistic insights obtained in this study should serve as useful and broadly applicable principles for future design of more efficient catalysts in fuel cells.

RESULTS AND DISCUSSION

Catalytic Four-Electron Reduction of O_2 by Fc and Me_2Fc with **1 in the Presence of HClO_4 .** The addition of a catalytic amount of **1** to an air-saturated acetone solution of

Me_2Fc and perchloric acid (HClO_4) results in the efficient reduction of O_2 by Me_2Fc to afford the corresponding dimethylferrocenium cation (Me_2Fc^+). The spectral changes for the catalytic reduction of O_2 by Me_2Fc with **1** in the presence of HClO_4 in acetone at 298 K are shown in Figure S1 [see Supporting Information (SI)]. When more than 4 equiv of Me_2Fc relative to O_2 (limiting $[\text{O}_2]$) was employed, 4 equiv of Me_2Fc^+ ($\lambda_{\text{max}} = 650 \text{ nm}$, $\epsilon = 360 \text{ M}^{-1} \text{ cm}^{-1}$) were formed in the presence of excess HClO_4 (Figure 1). From iodometric

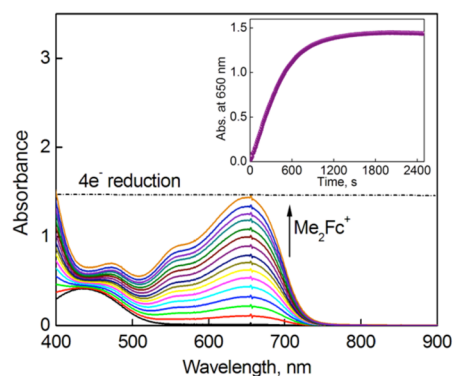


Figure 1. UV-vis spectral changes observed in the four-electron reduction of O_2 (1.0 mM) by Me_2Fc (6.0 mM) with HClO_4 (40 mM) catalyzed by **1** (0.20 mM) in acetone at 298 K. Inset shows the time profile of the absorbance at 650 nm due to Me_2Fc^+ .

titration experiments, it was confirmed that no H_2O_2 had formed after completion of the reaction (Figure S2 in SI). Thus, the four-electron reduction of O_2 by Me_2Fc occurs efficiently with a catalytic amount of **1** in the presence of HClO_4 (eq 2).



When Me_2Fc was replaced by the weaker reductant, Fc , the four-electron reduction of O_2 by Fc also occurred efficiently with **1** (Figure S3 in SI). The rate of formation of Me_2Fc^+ and Fc^+ obeyed pseudo-first-order kinetics under the conditions that $[\mathbf{1}] \ll [\text{O}_2] < [\text{Me}_2\text{Fc}] < [\text{HClO}_4]$ (Figure 1 inset). The time profiles of the absorbance at 650 nm due to Me_2Fc^+ and at 620 nm due to Fc^+ and the first-order plots by varying HClO_4 , O_2 , and catalyst are shown in SI, Figures S4, S5, S6a, and Figure 2a, respectively. The pseudo-first-order rate constant (k_{obs})

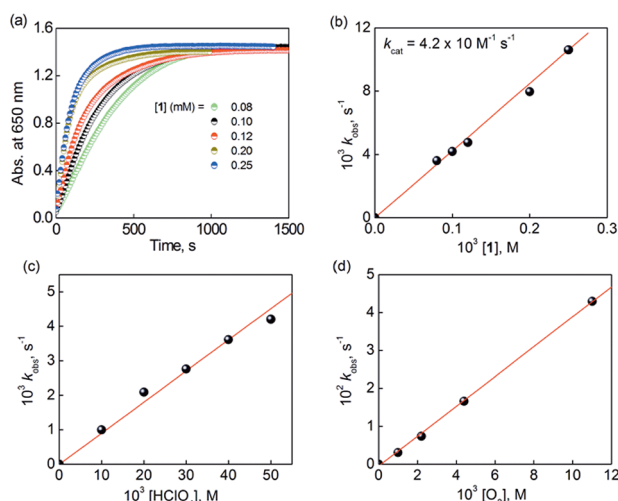


Figure 2. (a) Time profiles of the absorbance at 650 nm due to Me_2Fc^+ in the four-electron reduction of O_2 catalyzed by **1** (0.080 mM (green), 0.10 mM (black), 0.12 mM (red), 0.20 mM (dark yellow), and 0.25 mM (blue)) with Me_2Fc (4.0 mM) in the presence of HClO_4 (40 mM) in an air-saturated ($[\text{O}_2] = 2.2$ mM) acetone solution at 298 K. (b) Plot of k_{obs} vs $[\mathbf{1}]$ for the four-electron reduction of O_2 catalyzed by **1** with Me_2Fc (4.0 mM) in the presence of HClO_4 (40 mM) in an air-saturated ($[\text{O}_2] = 2.2$ mM) acetone solution at 298 K. (c) Plot of k_{obs} vs $[\text{HClO}_4]$ for the four-electron reduction of O_2 by Me_2Fc (4.0 mM) catalyzed by **1** (0.12 mM) in an acetone solution containing O_2 (2.2 mM) at 298 K. (d) Plot of k_{obs} vs $[\text{O}_2]$ for the four-electron reduction of O_2 catalyzed by **1** (0.20 mM) with Me_2Fc (3.2 mM) in the presence of HClO_4 (40 mM) in an acetone solution at 298 K.

increased linearly with increasing concentration of **1** (Figures 2b and S6b in SI). It should be noted that no oxidation of Me_2Fc occurs by O_2 in the presence of HClO_4 without **1**, under the present experimental conditions, even though ferrocene derivatives are known to be slowly oxidized by O_2 in the presence of strong acids.^{39,40} It should also be noted that the use of a noncoordinating solvent (acetone) is essential for the catalytic reduction of O_2 by Me_2Fc with **1** in the presence of HClO_4 , because a coordinating solvent such as acetonitrile prohibits such chemistry. The k_{obs} values were also proportional to concentrations of HClO_4 (Figures 2c and S6c in SI) and O_2 (Figures 2d and S6d in SI). Thus, the kinetic equation is given by eqs 3 and 4, where k_{cat} is the apparent fourth-order rate

$$\frac{d[\text{Me}_2\text{Fc}^+]}{dt} = k_{\text{obs}}[\text{Me}_2\text{Fc}] \quad (3)$$

$$k_{\text{obs}} = k_{\text{cat}}[\mathbf{1}][\text{O}_2][\text{H}^+] \quad (4)$$

constant (k_{cat}) for the catalytic four-electron reduction of O_2 by Me_2Fc when k_{obs} is given by eq 4. The k_{cat} values of Me_2Fc and Fc are listed in Table S1 in SI. The kinetic formulation in eqs 3 and 4 obtained in this study is quite unique because the rate is

proportional to concentrations of not only **1** but also O_2 , HClO_4 , and Me_2Fc , in sharp contrast to the previously reported cases of Cu catalysis for O_2 reduction in which the rate was rather independent of O_2 or H^+ .^{36–38} In such a case, the rate-determining step in the catalytic cycle should involve the reactions of **1** with Me_2Fc , O_2 , and H^+ . In order to elucidate the catalytic mechanism that can explain such a unique kinetic formulation, we decided to examine each portion of the catalytic cycle, step by step.

Protonation of 1 to Produce Two Independent Cu Centers. The catalytic reduction of O_2 by Me_2Fc and Fc with **1** was made possible only by the presence of HClO_4 . The effect of protonation of **1** was first examined by the spectral titration of **1** with HClO_4 (Figure 3). The absorption band at 378 nm

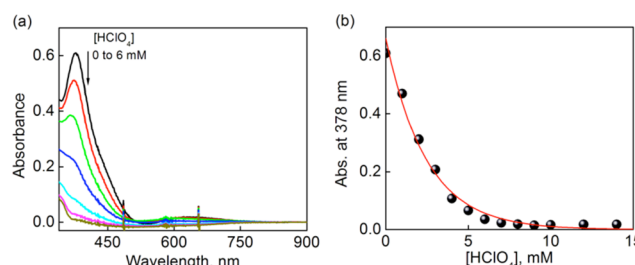
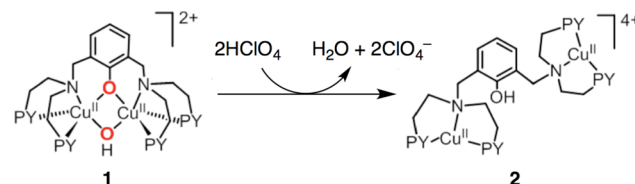


Figure 3. (a) UV–visible spectral changes of $[\text{Cu}^{\text{II}}_2(\text{XYLO})(\text{OH})](\text{PF}_6)_2$ (**1**) (0.20 mM) upon addition of HClO_4 (0.0–6.0 mM) in acetone at 298 K. (b) Absorbance changes at 378 nm as a function of HClO_4 concentration.

due to $[\text{Cu}^{\text{II}}_2(\text{XYLO})(\text{OH})]^{2+}$ decreased with increasing concentration of HClO_4 , and this was completely different from the spectral behavior of complex **1** with CF_3COOH (HOTF) where the absorption band was shifted to 420 nm and a clean isosbestic point was observed at 430 nm.³⁸ These spectral changes in the presence of HClO_4 indicate that not only the hydroxide group but also the phenoxo group of $[\text{Cu}^{\text{II}}_2(\text{XYLO})(\text{OH})]^{2+}$ (**1**) are protonated with HClO_4 , a much stronger acid than CF_3COOH , to produce $[\text{Cu}^{\text{II}}_2(\text{XYLOH})]^{4+}$ (**2**) (Scheme 2).

Scheme 2



The two-step protonation in Scheme 2 was confirmed by the EPR titration with HClO_4 . The starting dinuclear copper(II) complex $[\text{Cu}^{\text{II}}_2(\text{XYLO})(\text{OH})](\text{PF}_6)_2$ (**1**) is EPR silent because of antiferromagnetic coupling of the two Cu(II) ions (Figure 4a). It should be noted that, when the complex **1** was protonated with trifluoroacetic acid (HOTF), the protonated complex was EPR silent, indicating the two Cu(II) ions still maintain an electronic/magnetic interaction after the protonation of **1** with HOTF.³⁸ In the presence of one equiv of HClO_4 , which can protonate the OH group to produce H_2O , afforded the EPR silent species. In the presence of excess HClO_4 , however, a typical axial Cu(II) EPR spectroscopic signal was observed, indicating that both the hydroxide and the

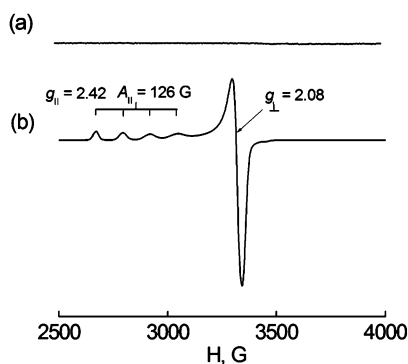


Figure 4. X-band EPR spectra of $[\text{Cu}^{\text{II}}_2(\text{XYLO})(\text{OH})](\text{PF}_6)_2$ (**1**) (1.0 mM) in the (a) absence and (b) presence of HClO_4 (5.0 mM) recorded in acetone at 5 K. The experimental parameters: microwave frequency = 9.646 GHz, microwave power = 1.0 mW, and modulation frequency = 100 kHz.

phenoxo group were protonated to produce two independent $\text{Cu}(\text{II})$ sites (Figure 4b).

Once the phenoxo group is protonated, the two Cu sites become independent and more electron deficient because of the lack of the coordination of the anionic phenoxo donor ligand. This was confirmed by the cyclic voltammetry (CV) and differential pulse voltammetry (DPV) measurements on **1** in the absence and presence of HClO_4 in acetone as shown in Figure 5. An irreversible cathodic peak current was observed at

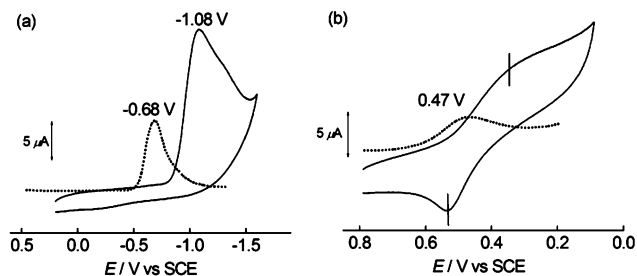


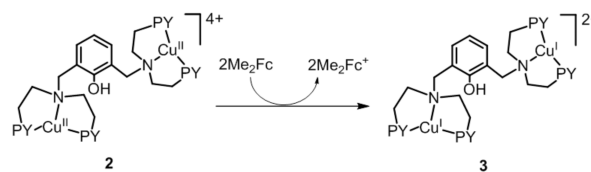
Figure 5. Cyclic voltammograms (CV, solid line) and differential pulse voltammograms (DPV, dotted line) of **1** (2.0 mM) in the (a) absence and (b) presence of HClO_4 (50 mM) in deaerated acetone at 298 K. TBAPF_6 (0.20 M) was used as an electrolyte.

−1.08 V vs SCE at a sweep rate of 0.10 V s^{-1} , whereas the DPV exhibits the cathodic peak at −0.68 V vs SCE. The cathodic peak is much more negative as compared to the one-electron oxidation potential of Me_2Fc ($E_{\text{ox}} = 0.26 \text{ V vs SCE}$) and Fc ($E_{\text{ox}} = 0.37 \text{ V vs SCE}$).^{31,41} This is the reason why no electron transfer from Me_2Fc or Fc to **1** occurs in the absence of acid. In the presence of HClO_4 , however, the one-electron reduction potential determined by DPV is shifted to the positive direction ($E_{\text{red}} = 0.47 \text{ V vs SCE}$) (Figure 5b) which is now more positive than the oxidation potential of Fc ($E_{\text{ox}} = 0.37 \text{ V vs SCE}$) and Me_2Fc ($E_{\text{ox}} = 0.26 \text{ V vs SCE}$). Thus, electron transfer from Fc and Me_2Fc to **1** becomes energetically feasible in the presence of HClO_4 . This was confirmed by examination of electron transfer from Fc and Me_2Fc to **1** in the presence of excess HClO_4 in acetone (vide infra).

Electron Transfer from Ferrocene Derivatives to **1 in the Presence of HClO_4 .** No electron transfer from Me_2Fc and Fc to $[\text{Cu}^{\text{II}}_2(\text{XYLO})(\text{OH})]^{2+}$ (**1**) occurs in the absence of HClO_4 in acetone at 298 K, whereas the electron transfer occurs to completion to produce the corresponding ferrocene-

nium ions in the presence of HClO_4 (Scheme 3). The rates of electron transfer from Me_2Fc and Fc to **1** were determined in

Scheme 3



the presence of HClO_4 at 298 K under an argon atmosphere. The rate of formation of Me_2Fc^+ and Fc^+ obeyed pseudo-first-order kinetics under the conditions that $[\text{HClO}_4] \gg [\text{Me}_2\text{Fc}]$ and $[\text{Fc}] > [\text{1}]$ as shown in Figure S8 (SI). The amount of Me_2Fc^+ produced by electron transfer from Me_2Fc to **1** in the presence of HClO_4 is twice that observed for complex **1** (0.10 mM). This result indicates that the two Cu sites of protonated **1** (Scheme 2) act independently without any interaction between them. The observed pseudo-first-order rate constant (k_{obs}) increased linearly with increasing concentration of Me_2Fc and Fc (Figure 6). The second-order rate constants (k_{et}) of

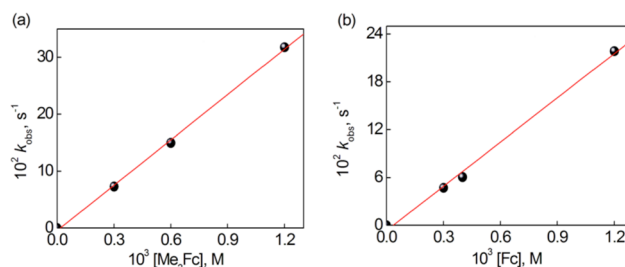


Figure 6. (a) Plot of k_{obs} vs $[\text{Me}_2\text{Fc}]$ in the electron transfer from Me_2Fc to $[\text{Cu}^{\text{II}}_2(\text{XYLO})(\text{OH})](\text{PF}_6)_2$ (**1**) (0.10 mM) in the presence of HClO_4 (40 mM) in acetone at 298 K. (b) Plot of k_{obs} vs $[\text{Fc}]$ in the electron transfer from Fc to **1** (0.10 mM) in the presence of HClO_4 (40 mM) in acetone at 298 K.

electron transfer from Me_2Fc and Fc to **1** at 298 K were determined to be $2.7 \times 10^2 \text{ M}^{-1} \text{ s}^{-1}$ and $1.8 \times 10^2 \text{ M}^{-1} \text{ s}^{-1}$ from the slopes of linear plots of k_{obs} vs $[\text{Me}_2\text{Fc}]$ and $[\text{Fc}]$, respectively. The k_{et} values are listed in Table S1 (SI) together with the k_{cat} values.

The k_{et} values ($2.7 \times 10^2 \text{ M}^{-1} \text{ s}^{-1}$ and $1.8 \times 10^2 \text{ M}^{-1} \text{ s}^{-1}$) of electron transfer from Me_2Fc and Fc to **1** in the presence of 40 mM HClO_4 are significantly larger than the corresponding $k_{\text{obs}}/[\text{1}]$ (see eqs 3 and 4) values ($42 \text{ M}^{-1} \text{ s}^{-1}$ in Figure 2b and $10 \text{ M}^{-1} \text{ s}^{-1}$ in Figure S6b [SI]) in the presence of 40 mM HClO_4 , respectively. Thus, the electron-transfer step is not the rate-determining step in the catalytic cycle. The electron transfer from Me_2Fc and Fc to **1** in the presence of excess HClO_4 without O_2 results in formation of the protonated dinuclear $\text{Cu}(\text{I})$ complex, $[\text{Cu}^{\text{I}}_2(\text{XYLOH})]^{2+}$, which can reduce O_2 . Next we examined the reaction of $[\text{Cu}^{\text{I}}_2(\text{XYLOH})]^{2+}$ with O_2 at low temperatures to detect any copper–dioxygen intermediate.

Reversible Binding of O_2 to $[\text{Cu}^{\text{I}}_2(\text{XYLOH})]^{2+}$. When O_2 was bubbled into an acetone solution of separately synthesized dicopper(I) complex, $[\text{Cu}^{\text{I}}_2(\text{XYLOH})]^{2+}$ at 193 K, the absorption band at 395 nm due to the hydroperoxo complex, $[\text{Cu}^{\text{II}}_2(\text{XYLO})(\text{OOH})]^{2+}$,⁴⁷ appeared immediately as shown in Figure 7 and Scheme 4. The yield of hydroperoxo complex, $[\text{Cu}^{\text{II}}_2(\text{XYLO})(\text{OOH})]^{2+}$ (**4**) was determined to be 100% at

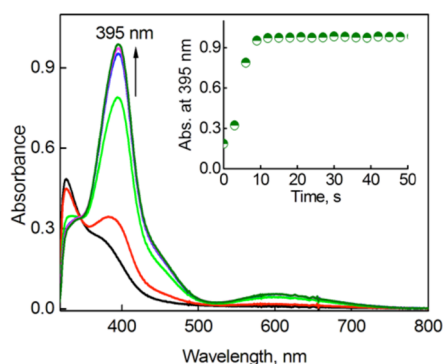
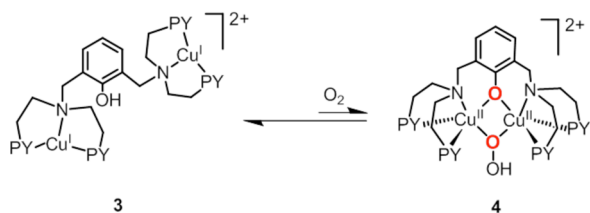


Figure 7. Formation of the hydroperoxo complex, $[\text{Cu}^{\text{II}}_2(\text{XYLO})(\text{OOH})]^{2+}$ ($\lambda_{\text{max}} = 395 \text{ nm}$) in the reaction of $[\text{Cu}^{\text{I}}_2(\text{XYLOH})]^{2+}$ (0.11 mM) with O_2 in acetone at 193 K.

Scheme 4



193 K. As the temperature increased, the absorption band at 395 nm due to $[\text{Cu}^{\text{II}}_2(\text{XYLO})(\text{OOH})]^{2+}$ decreased. This process was reversible at low temperatures up to 223 K (Figure 8a).⁴² The temperature dependence of K_{eq} was examined

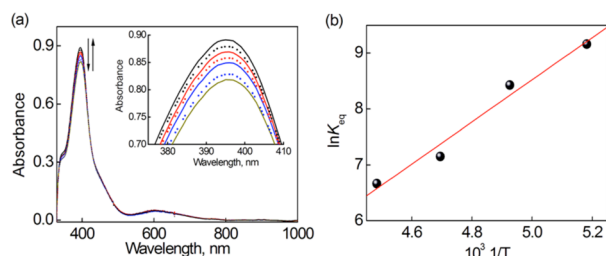


Figure 8. (a) UV–visible spectra indicating the reversible nature of dioxxygen binding to $[\text{Cu}^{\text{I}}_2(\text{XYLOH})]^{2+}$ (**3**). Bubbling O_2 into an acetone solution of **3** produces $[\text{Cu}^{\text{II}}_2(\text{XYLO})(\text{OOH})]^{2+}$ (**4**) at 193 K (black, solid line) (inset zoom view). Increasing the temperature up to 223 K produces dark-yellow solid spectrum. After cooling to 193 K again gives black dotted spectrum. (b) van't Hoff plot to determine the activation parameters, enthalpy and entropy, in the dioxxygen binding to $[\text{Cu}^{\text{I}}_2(\text{XYLOH})]^{2+}$ in acetone.

(Figure S9 in SI), and the van't Hoff plot (Figure 8b) afforded $\Delta H = -31 \text{ kJ mol}^{-1}$ and $\Delta S = -86 \text{ J K}^{-1} \text{ mol}^{-1}$. The equilibrium constant at 298 K was estimated to be 11 M^{-1} from the extrapolation of the van't Hoff plot. The equilibrium lies to the reactant side at 298 K when only a small portion of $[\text{Cu}^{\text{I}}_2(\text{XYLOH})]^{2+}$ is converted to $[\text{Cu}^{\text{II}}_2(\text{XYLO})(\text{OOH})]^{2+}$ (~10%).

This intermediate was further reduced by decamethylferrocene (Fc^*) in the presence of HClO_4 at 193 K (Scheme 5, Figure 9). Fc^* was used because the reactions with Me_2Fc and Fc were too slow to be followed at 193 K.

An alternate reaction pathway that may contribute in a small way to the overall chemistry and catalytic cycle comes about if the hydroperoxo complex $[\text{Cu}^{\text{II}}_2(\text{XYLO})(\text{OOH})]^{2+}$ (**4**) is

Scheme 5

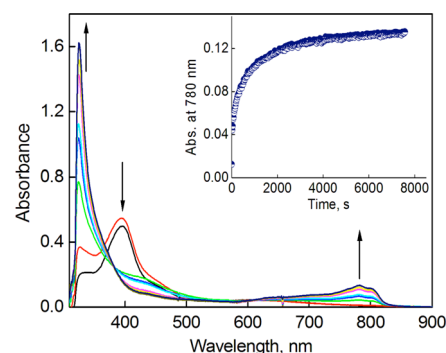
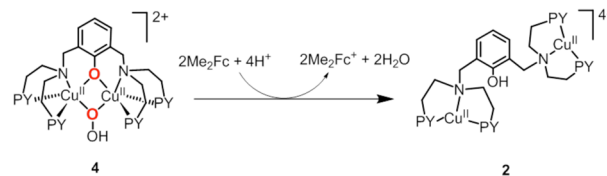
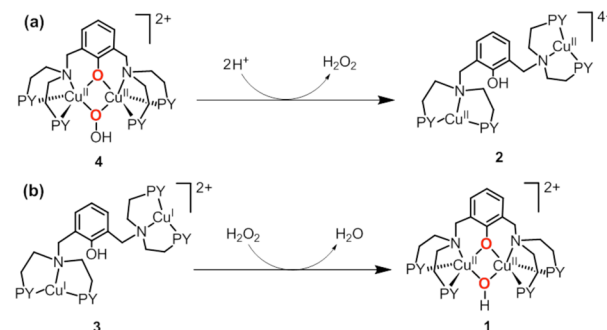


Figure 9. Formation of Fc^{*+} by addition of Fc^* (0.25 mM) and HClO_4 (40 mM) to the hydroperoxo complex (0.060 mM) (generated by O_2 bubbling to the solution of $[\text{Cu}^{\text{I}}_2(\text{XYLOH})]^{2+}$ (0.060 mM)) at 193 K.

protonated in the presence of HClO_4 to yield hydrogen peroxide and protonated dicopper(II) complex, $[\text{Cu}^{\text{II}}_2(\text{XYLOH})]^{4+}$ (**2**) (Scheme 6a). This was separately

Scheme 6



demonstrated using excess HClO_4 (10 equiv) (Figure S10 in SI). However, we find that if hydrogen peroxide forms in this manner, it would be readily reduced to H_2O by the dicopper(I) complex $[\text{Cu}^{\text{I}}_2(\text{XYLOH})]^{2+}$ (**3**) (Scheme 6b and Figure 10; see also Figure S11 in SI). Although H_2O_2 and $\text{Cu}(\text{II})\text{-H}_2\text{O}_2$ adducts have been previously reported to react directly with acetone,^{43,44} clean and fast conversion of **3** with H_2O_2 to **1** in Figure 10 suggests the reaction of H_2O_2 and the Cu complex with acetone may be negligible under the present reaction conditions. The observed first-order rate constant (k_{obs}) increased linearly with increasing concentration of H_2O_2 (Figure 10b). The second-order rate constant (k_2) was determined to be $2.5 \times 10^3 \text{ M}^{-1} \text{ s}^{-1}$ at 298 K, which is much larger than the $k_{\text{obs}}/[1]$ values (vide supra). Thus, under the catalytic conditions, the H_2O_2 produced, if any, is rapidly reduced by $[\text{Cu}^{\text{I}}_2(\text{XYLOH})]^{2+}$, contributing to the overall four-electron four-proton reduction of O_2 .

The overall catalytic cycle is summarized in Scheme 7. The protonation of $[\text{Cu}^{\text{II}}_2(\text{XYLO})(\text{OH})]^{2+}$ (**1**) results in formation

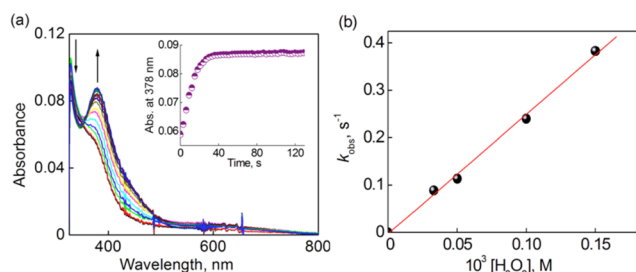
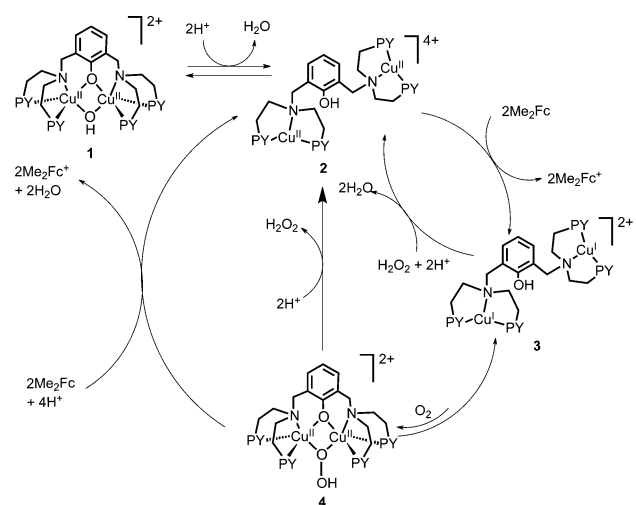


Figure 10. (a) UV-vis spectral changes observed in the reaction of H_2O_2 (0.033 mM) with $[\text{Cu}_2(\text{XYLOH})]^{2+}$ (0.025 mM) in acetone at 298 K. Inset shows the time profile monitored at 378 nm due to the formation of $[\text{Cu}^{\text{II}}_2(\text{XYLO})(\text{OH})]^{2+}$. (b) Plot of k_{obs} vs $[\text{H}_2\text{O}_2]$ in the reaction of H_2O_2 with $[\text{Cu}_2(\text{XYLOH})]^{2+}$ (0.025 mM) in acetone at 298 K.

Scheme 7



of $[\text{Cu}_2(\text{XYLOH})]^{4+}$ (2), which can be reduced by two equiv of Fc and Me_2Fc to produce fully reduced dicopper(I) complex $[\text{Cu}_2(\text{XYLOH})]^{2+}$ (3). The O_2 -binding to (3) to produce hydroperoxo complex $[\text{Cu}_2(\text{XYLO})(\text{OOH})]^{2+}$ (4) is an equilibrium process. At 298 K, only a small portion of $[\text{Cu}_2(\text{XYLOH})]^{2+}$ is converted to $[\text{Cu}_2(\text{XYLO})(\text{OOH})]^{2+}$, the concentration of which is proportional to the O_2 concentration. $[\text{Cu}_2(\text{XYLO})(\text{OOH})]^{2+}$ that is formed undergoes further reduction by PCET from Fc and Me_2Fc , leading to the four-electron reduction of O_2 . In this final two-electron peroxide reduction, the first PCET reduction may be the rate-determining step followed by the much faster second PCET reduction to produce H_2O . In such a case, the overall catalytic rate is proportional to concentrations of 1, O_2 , HClO_4 , and electron donors (Fc and Me_2Fc) as observed in Figure 2 and Figures S4–S6 in SI. The PCET reduction of $[\text{Cu}_2(\text{XYLO})(\text{OOH})]^{2+}$ may compete with the protonation of $[\text{Cu}_2(\text{XYLO})(\text{OOH})]^{2+}$ (4) to generate H_2O_2 (Scheme 6); however, H_2O_2 thus produced is rapidly reduced to H_2O by $[\text{Cu}_2(\text{XYLOH})]^{2+}$ (vide supra).

According to Scheme 7, the equilibrium between $[\text{Cu}_2(\text{XYLOH})]^{2+}$ (3) with O_2 and $[\text{Cu}_2(\text{XYLO})(\text{OOH})]^{2+}$ (4) at 298 K lies to the side of $[\text{Cu}_2(\text{XYLOH})]^{2+}$ (vide infra), the $[\text{Cu}_2(\text{XYLOH})]^{4+}$ complex is being converted to $[\text{Cu}_2(\text{XYLOH})]^{2+}$ during the catalytic reaction but $[\text{Cu}_2(\text{XYLOH})]^{4+}$ (2) may be regenerated after the completion of the catalytic reaction when all ferrocenes were

consumed. This was confirmed as the change in the EPR spectra as shown in Figure 11, where the EPR signal due to

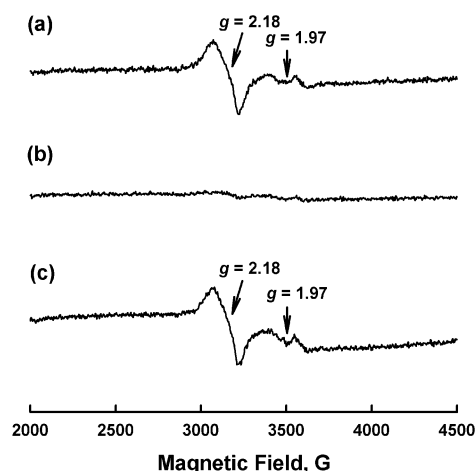


Figure 11. EPR spectra of (a) $[\text{Cu}_2(\text{XYLO})(\text{OH})](\text{PF}_6)_2$ (1) (0.040 mM) with HClO_4 (40 mM) and (b, c) the reaction solution of 1 (0.040 mM) with Me_2Fc (10 mM) in the presence of HClO_4 (40 mM) in O_2 -saturated acetone at 298 K [(b) during the reaction and (c) after completion of the reaction]. Spectra were recorded at 20 K. The experimental parameters: microwave frequency = 9.654 GHz, microwave power = 1.0 mW, and modulation frequency = 100 kHz.

$[\text{Cu}_2(\text{XYLOH})]^{4+}$ (2) observed before the reaction disappeared during the catalytic reaction but reappeared after completion of the reaction without exhibiting any decomposition.

The kinetic results (as described by eqs 3 and 4) and the absence of the EPR signal due to 2 during the catalytic reaction indicate that the reaction of 3 with O_2 , Me_2Fc and H^+ involves all of these species in the rate-determining step. As described above, we have also separately shown that 4 is formed by the reaction of 2 and O_2 at 193 K (Figure 7).⁴⁷ At 298 K, the equilibrium for the formation of 4 lies to 2 (vide supra), when the concentration of 4 may be proportional to $[\text{O}_2]$. Then, the PCET reduction of 4 by Me_2Fc may compete with the formation of H_2O_2 by the protonation of 4. At 193 K, the protonation of 4 to produce H_2O_2 may be the major pathway as indicated by the results in Figure 9. At 298 K, however, the PCET reduction of 4 by Me_2Fc may be the major pathway when the rate of formation of Me_2Fc^+ is derived as given by eq 5, where k_{PCET} is the rate constant of PCET reduction of 4

$$\frac{d[\text{Me}_2\text{Fc}^+]}{dt} = k_{\text{PCET}}K[\text{Me}_2\text{Fc}][1][\text{O}_2][\text{H}^+] \quad (5)$$

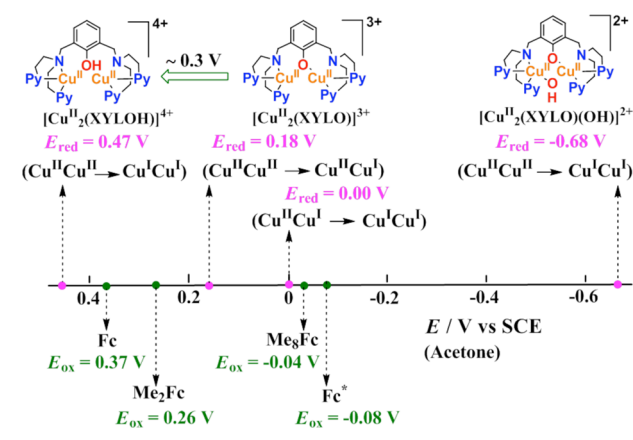
and K is the equilibrium constant of formation of 4 with O_2 from 3. The derived kinetic equation (eq 5) agrees with the experimental observations in eqs 3 and 4. If the protonation of 4 to produce H_2O_2 was the major pathway at 298 K, the rate would not be dependent on Me_2Fc , because electron transfer from Me_2Fc to 2 was shown to be too fast to be involved in the rate-determining step. Because the rate is proportional to $[\text{Me}_2\text{Fc}]$, the rate-determining step must be the PCET reduction of 4 by Me_2Fc . It should be noted that the protonation of 1 is completed in the presence of HClO_4 (>10 mM) as shown in Figure 2, when the linear dependence of the rate on concentration of HClO_4 (>10 mM) in Figure 2c results from the rate-determining PCET reduction of 4.

CONCLUSION

A dinuclear copper(II) complex ($[\text{Cu}^{\text{II}}_2(\text{XYLO})(\text{OH})]^{2+}$) acts as an efficient catalyst for the four-electron reduction of O_2 by Me_2Fc and Fc with HClO_4 in acetone as shown in Scheme 7. The hydroxide group as well as the phenoxo group of $[\text{Cu}^{\text{II}}_2(\text{XYLO})(\text{OH})]^{2+}$ (1) were protonated with HClO_4 to produce $[\text{Cu}^{\text{II}}_2(\text{XYLOH})]^{4+}$ (2) which can be reduced by Me_2Fc and Fc to produce $[\text{Cu}^{\text{I}}_2(\text{XYLOH})]^{2+}$ (3). The dinuclear Cu(I) complex $[\text{Cu}^{\text{I}}_2(\text{XYLOH})]^{2+}$ (3) reacts with O_2 to produce the hydroperoxo complex ($[\text{Cu}^{\text{II}}_2(\text{XYLO})(\text{OOH})]^+$ (4)), and this is followed by PCET reduction, leading to the catalytic four-electron reduction of O_2 by Fc and Me_2Fc .

It is instructive to compare and contrast the chemistry described here with that previously reported,³⁸ both with exactly the same catalyst, $[\text{Cu}^{\text{II}}_2(\text{XYLO})(\text{OH})]^{2+}$ (1) (Schemes 1 and 8) but having very differing behaviors. As indicated in the

Scheme 8



summary in Scheme 8, 1 is quite difficult to reduce, but in the presence of HClO_4 , the bridging hydroxide ligand is displaced (as H_2O) and now, reduction to a dicopper(I) (or a mixed-valent form, $[\text{Cu}^{\text{II}}\text{Cu}^{\text{I}}(\text{XYLO})]^{2+}$),³⁸ is possible; it is this/these forms which are required for O_2 -binding and initial reduction to the peroxide level.

With HOTF, however, the phenoxo O-atom still bridges the Cu(II) ions, leaving the redox potential negative enough to require stronger reductants such as Me_8Fc or Fc^* . A key coordination chemistry aspect is that HClO_4 as proton source is strong enough to break the phenoxide bridge between copper ions, allowing facile reduction of the Cu(II) ions with Me_2Fc or even Fc itself; the complex produced, $[\text{Cu}^{\text{II}}_2(\text{XYLOH})]^{4+}$ (2), now has Cu(II) ions possessing only N_3 -bis[(2-(2-pyridyl)-ethyl)amine] chelation (Scheme 8). Thus, the change to perchloric acid facilitates a drop in effective overpotential of ~ 0.30 V, or more (Scheme 8).

Perchloric acid effects another dramatic change; the reaction mechanism switches from the catalytic two-electron two-proton reduction of O_2 to H_2O_2 with HOTF, to the catalytic four-electron four-proton reduction of O_2 to water with HClO_4 . First, for the HOTF case, dicopper(II) reduction is rate limiting, but with HClO_4 , PCET reduction/protonation of $[\text{Cu}^{\text{II}}_2(\text{XYLO})(\text{OOH})]^{2+}$ (4) is the rate-determining step. Second, note that in both systems, the hydroperoxo complex 4 is the key oxygen intermediate which is formed. HOTF readily protonates off the bound $-\text{OOH}$ ligand giving H_2O_2 ,

but it is not strong enough to allow PCET hydroperoxide reduction to water. Perchloric acid does facilitate the latter hydroperoxide reductive cleavage to water, accounting for the differing stoichiometries of catalytic O_2 -reduction chemistry.

Although the mechanism of the PCET reduction of 4 by Me_2Fc has yet to be clarified, the chemistry described here provides the first example of four-electron reduction of O_2 by one-electron reductants weaker than Fc^* such as Fc and Me_2Fc in the presence of HClO_4 in acetone by a copper complex acting as a catalyst. The present study opens a new approach to achieve less overpotential which is more desirable and more energy efficient for the catalytic four-electron reduction of O_2 using copper complexes.

EXPERIMENTAL SECTION

Materials. Grade-quality solvents and chemicals were obtained commercially and used without further purification unless otherwise noted. Decamethylferrocene (Fc^*) (97%), 1,1'-dimethylferrocene (Me_2Fc), ferrocene (Fc), hydrogen peroxide (30%), and HClO_4 (70%) were purchased from Aldrich Co., U.S., and NaI (99.5%) was from Junsei Chemical Co., Japan. Acetone was purchased from JT Baker, U.S., and used either without further purification for nonair-sensitive experiments or dried and distilled under argon and then deoxygenated by bubbling with argon for 30–45 min and kept over activated molecular sieve (4 Å) for air-sensitive experiments.⁴⁵ Preparation and handling of air-sensitive compounds were performed under Ar atmosphere (<1 ppm O_2 and <1 ppm H_2O) in a glovebox (Korea Kiyon Co., Ltd.). The copper complexes, $[\text{Cu}^{\text{I}}_2(\text{XYLH})(\text{CH}_3\text{CN})_2](\text{PF}_6)_2$ (XYLH = *m*-xylene-linked bis[(2-(2-pyridyl)ethyl)amine]),⁴⁶ which is a precursor complex, $[\text{Cu}^{\text{II}}_2(\text{XYLO})(\text{OH})](\text{PF}_6)_2$ (1), and $[\text{Cu}^{\text{I}}_2(\text{XYLOH})](\text{PF}_6)_2$, were prepared according to the literature procedures.⁴⁷

Instrumentation. UV-vis spectra were recorded on a Hewlett-Packard 8453 diode array spectrophotometer equipped with a UNISOKU Scientific Instruments Cryostat USP-203A for low-temperature experiments or a UNISOKU RSP-601 stopped-flow spectrometer equipped with a MOS-type highly sensitive photodiode array. Cyclic voltammetry (CV) and differential pulse voltammetry (DPV) measurements were performed on an ALS 630B electrochemical analyzer, and voltammograms were measured in deaerated acetone containing 0.20 M TBAPF₆ as a supporting electrolyte at room temperature. A conventional three-electrode cell was used with a gold working electrode (surface area of 0.3 mm²), and a platinum wire was the counter electrode. The gold working electrode was routinely polished with BAS polishing alumina suspension and rinsed with acetone before use. The potentials were measured with respect to the Ag/AgNO₃ (10 mM) reference electrode and were converted to values vs SCE by adding 0.29 V.⁴⁸ All electrochemical measurements were carried out under an atmospheric pressure of nitrogen. X-band EPR spectra were recorded at 5 or 20 K using an X-band Bruker EMX-plus spectrometer equipped with a dual mode cavity (ER 4116DM). Low temperature was achieved and controlled with an Oxford Instruments ESR900 liquid helium quartz cryostat with an Oxford Instruments ITC503 temperature and gas flow controller. The experimental parameters for EPR spectra were as follows: microwave frequency = 9.646 GHz at 5 K and 9.654 GHz at 20 K, microwave power = 1.0 mW, modulation amplitude = 10 G, gain = 5×10^3 , modulation frequency = 100 kHz, time constant = 81.92 ms, and conversion time = 81.00 ms.

Kinetic Measurements. The UV-vis spectral changes were recorded on a Hewlett-Packard 8453 diode array spectrophotometer equipped with Unisoku thermostatted cell holder for low-temperature experiments. Rate constants in the oxidation reaction of ferrocene derivatives by O_2 in the presence of catalytic amount of 1 and excess amount of perchloric acid (HClO_4) in acetone at 298 K were determined by monitoring the appearance of the absorption band due to the corresponding ferrocenium ions (Fc^+ : $\lambda_{\text{max}} = 620$ nm, $\epsilon_{\text{max}} = 430$ M⁻¹ cm⁻¹; Me_2Fc^+ : $\lambda_{\text{max}} = 650$ nm; $\epsilon_{\text{max}} = 360$ M⁻¹ cm⁻¹; Fc^{*+} : $\lambda_{\text{max}} =$

780 nm; $\epsilon_{\text{max}} = 520 \text{ M}^{-1} \text{ cm}^{-1}$). The limiting concentration of O_2 in an acetone solution was prepared by a mixed-gas flow of O_2 and Ar. The mixed gas was controlled by using a gas mixer (SMTEK, Korea), which can mix O_2 and Ar gases at a certain pressure and flow rate for the rate measurements with the different concentrations of O_2 in Figure 2c. The rate constants as determined from the first-order plots are provided in the SI (Table S1).

Spectroscopic Measurements. The amount of H_2O_2 was determined by titration with iodide ion.⁴⁹ The diluted acetone solution of the reduced product of O_2 was treated with an excess of NaI. The amount of I_3^- formed was then quantified using its visible spectrum ($\lambda_{\text{max}} = 361 \text{ nm}$; $\epsilon = 2.5 \times 10^4 \text{ M}^{-1} \text{ cm}^{-1}$).

Low-Temperature Experiments Concerning the Generation of $[\text{Cu}^{\text{II}}(\text{XYLO})(\text{OOH})]^{2+}$ (4). Under an argon atmosphere within a glovebox, $[\text{Cu}^{\text{I}}(\text{XYLOH})](\text{PF}_6)_2$ (0.11 mM) was dissolved in 3.0 mL of O_2 -free acetone. The cuvette was fully sealed with a septum and quickly removed from the glovebox and cooled to -80°C in the UV-vis spectrophotometer equipped with a thermostatted cell holder. O_2 was gently bubbled through the reaction solution, and the formation of the hydroperoxo species was followed by the change in the absorbance at 395 nm.

■ ASSOCIATED CONTENT

■ Supporting Information

Figures S1–S11 and Table S1. This material is available free of charge via the Internet at <http://pubs.acs.org>.

■ AUTHOR INFORMATION

Corresponding Author

fukuzumi@chem.eng.osaka-u.ac.jp (S.F.); karlin@jhu.edu (K.D.K.); wwnam@ewha.ac.kr (W.N.).

Notes

The authors declare no competing financial interest.

■ ACKNOWLEDGMENTS

This work was supported by Grants-in-Aid (Scientific Research on Innovative Areas, No. 20108010 to S.F., 23750014 to K.O. and by NRF/MEST of Korea through CRI (to W.N.), GRL (2010-00353) (to W.N.), and WCU (R31-2008-000-10010-0) (to W.N., S.F., and K.D.K.). K.D.K. also acknowledges support from the United States National Institutes of Health Grant, GM28962.

■ REFERENCES

- (1) (a) Pereira, M. M.; Santana, M.; Teixeira, M. *Biochim. Biophys. Acta* **2001**, 1505, 185. (b) Tsukihara, T.; Aoyama, H.; Yamashita, E.; Tomizaki, T.; Yamaguchi, H.; Shinzawa-Itoh, K.; Nakashima, R.; Yaono, R.; Yoshikawa, S. *Science* **1995**, 269, 1069. (c) Yoshikawa, S.; Shinzawa-Itoh, K.; Nakashima, R.; Yaono, R.; Yamashita, E.; Inoue, N.; Yao, M.; Fei, M. J.; Libeu, C. P.; Mizushima, T.; Yamaguchi, H.; Tomizaki, T.; Tsukihara, T. *Science* **1998**, 280, 1723.
- (2) (a) Malmström, B. G. *Acc. Chem. Res.* **1993**, 26, 332. (b) Malmström, B. G. *Chem. Rev.* **1990**, 90, 1247. (c) Winter, M.; Brodd, R. J. *Chem. Rev.* **2004**, 104, 4245.
- (3) (a) Ferguson-Miller, S.; Babcock, G. T. *Chem. Rev.* **1996**, 96, 2889. (b) Hosler, J. P.; Ferguson-Miller, S.; Mills, D. A. *Annu. Rev. Biochem.* **2006**, 75, 165. (c) Kaila, V. R. I.; Verkhovsky, M. I.; Wikström, M. *Chem. Rev.* **2010**, 110, 7062.
- (4) (a) Kim, E.; Chufan, E. E.; Kamaraj, K.; Karlin, K. D. *Chem. Rev.* **2004**, 104, 1077. (b) Chufan, E. E.; Pui, S. C.; Karlin, K. D. *Acc. Chem. Res.* **2007**, 40, 563. (c) Collman, J. P.; Boulatov, R.; Sunderland, C. J.; Fu, L. *Chem. Rev.* **2004**, 104, 561.
- (5) Babcock, G. T.; Wikström, M. *Nature* **1992**, 356, 301.
- (6) (a) Stambouli, A. B.; Traversa, E. *Renew. Sust. Energy Rev.* **2002**, 6, 295. (b) Marković, N. M.; Schmidt, T. J.; Stamenković, V.; Ross, P. N. *Fuel Cells* **2001**, 1, 105. (c) Steele, B. C. H.; Heinzel, A. *Nature* **2001**, 414, 345.
- (7) Borup, R.; Meyers, J.; Pivovar, B.; Kim, Y. S.; Mukundan, R.; Garland, N.; Myers, D.; Wilson, M.; Garzon, F.; Wood, D.; Zelenay, P.; More, K.; Stroh, K.; Zawodzinski, T.; Boncella, J.; McGrath, J. E.; Inaba, M.; Miyatake, K.; Hori, M.; Ota, K.; Ogumi, Z.; Miyata, S.; Nishikata, A.; Siroma, Z.; Uchimoto, Y.; Yasuda, K.; Kimijima, K.-i.; Iwashita, N. *Chem. Rev.* **2007**, 107, 3904.
- (8) (a) Cracknell, J. A.; Vincent, K. A.; Armstrong, F. A. *Chem. Rev.* **2008**, 108, 2439. (b) Willner, I.; Yan, Y.-M.; Willner, B.; Tel-Vered, R. *Fuel Cells* **2009**, 9, 7.
- (9) Shin, H.; Lee, D.-H.; Kang, C.; Karlin, K. D. *Electrochim. Acta* **2003**, 48, 4077.
- (10) (a) Lee, K.; Zhang, L.; Zhang, J. *PEM Fuel Cell Electrocatalysts and Catalyst Layers*; Springer: London, 2008; p 715. (b) Anson, F. C.; Shi, C.; Steiger, B. *Acc. Chem. Res.* **1997**, 30, 437.
- (11) (a) Wang, B. J. *Power Sources* **2005**, 152. (b) Peljo, P.; Rauhala, T.; Murtomäki, L.; Kallio, T.; Kontturi, K. *Int. J. Hydrogen Energy* **2011**, 36, 10033.
- (12) (a) Collman, J. P.; Devaraj, N. K.; Decréau, R. A.; Yang, Y.; Yan, Y.-L.; Ebina, W.; Eberspacher, T. A.; Chidsey, C. E. D. *Science* **2007**, 315, 1565. (b) Collman, J. P.; Decréau, R. A.; Lin, H.; Hosseini, A.; Yang, Y.; Dey, A.; Eberspacher, T. A. *Proc. Natl. Acad. Sci. U.S.A.* **2009**, 106, 7320. (c) Collman, J. P.; Ghosh, S.; Dey, A.; Decréau, R. A.; Yang, Y. *J. Am. Chem. Soc.* **2009**, 131, 5034.
- (13) (a) Kadish, K. M.; Frémond, L.; Shen, J.; Chen, P.; Ohkubo, K.; Fukuzumi, S.; El Ojaimi, M.; Gros, C. P.; Barbe, J.-M.; Guillard, R. *Inorg. Chem.* **2009**, 48, 2571. (b) Kadish, K. M.; Shen, J.; Frémond, L.; Chen, P.; Ojaimi, M. E.; Chkounda, M.; Gros, C. P.; Barbe, J.-M.; Ohkubo, K.; Fukuzumi, S.; Guillard, R. *Inorg. Chem.* **2008**, 47, 6726. (c) Ou, Z.; Lü, A.; Meng, D.; Huang, S.; Fang, Y.; Lu, G.; Kadish, K. M. *Inorg. Chem.* **2012**, 51, 8890.
- (14) (a) Chen, W.; Akhigbe, J.; Brückner, C.; Li, C. M.; Lei, Y. J. *Phys. Chem. C* **2010**, 114, 8633. (b) Kadish, K. M.; Frémond, L.; Ou, Z.; Shao, J.; Shi, C.; Anson, F. C.; Burdet, F.; Gros, C. P.; Barbe, J. M.; Guillard, R. *J. Am. Chem. Soc.* **2005**, 127, 5625.
- (15) (a) Rosenthal, J.; Nocera, D. G. *Acc. Chem. Res.* **2007**, 40, 543. (b) Chang, C. J.; Loh, Z.-H.; Shi, C.; Anson, F. C.; Nocera, D. G. *J. Am. Chem. Soc.* **2004**, 126, 10013.
- (16) (a) Dogutan, D. K.; Stoian, S. A.; McGuire, R.; Schwalbe, M.; Teets, T. S.; Nocera, D. G. *J. Am. Chem. Soc.* **2011**, 133, 131. (b) Teets, T. S.; Cook, T. R.; McCarthy, B. D.; Nocera, D. G. *J. Am. Chem. Soc.* **2011**, 133, 8114.
- (17) (a) Carver, C. T.; Matson, B. D.; Mayer, J. M. *J. Am. Chem. Soc.* **2012**, 134, 5444. (b) Samanta, S.; Sengupta, K.; Mittra, K.; Bandyopadhyay, S.; Dey, A. *Chem. Commun.* **2012**, 48, 7631.
- (18) Fukuzumi, S.; Yamada, Y.; Karlin, K. D. *Electrochim. Acta* **2012**, 82, 493.
- (19) (a) Li, W.; Yu, A.; Higgins, D. C.; Llanos, B. G.; Chen, Z. *J. Am. Chem. Soc.* **2010**, 132, 17056. (b) Ward, A. L.; Elbaz, L.; Kerr, J. B.; Arnold, J. *Inorg. Chem.* **2012**, 51, 4694.
- (20) (a) Zhang, J.; Anson, F. C. *J. Electroanal. Chem.* **1992**, 341, 323. (b) Zhang, J.; Anson, F. C. *J. Electroanal. Chem.* **1993**, 348, 81.
- (21) (a) Zhang, J.; Anson, F. C. *Electrochim. Acta* **1993**, 38, 2423. (b) Lei, Y.; Anson, F. C. *Inorg. Chem.* **1994**, 33, 5003.
- (22) (a) Weng, Y. C.; Fan, F.-R. F.; Bard, A. J. *J. Am. Chem. Soc.* **2005**, 127, 17576. (b) Thorum, M. S.; Yadav, J.; Gewirth, A. A. *Angew. Chem., Int. Ed.* **2009**, 48, 165.
- (23) (a) McCrory, C. C. L.; Ottenwaelde, X.; Stack, T. D. P.; Chidsey, C. E. D. *J. Phys. Chem. A* **2007**, 111, 12641. (b) McCrory, C. C. L.; Devadoss, A.; Ottenwaelde, X.; Lowe, R. D.; T. Stack, T. D. P.; Chidsey, C. E. D. *J. Am. Chem. Soc.* **2011**, 133, 3696.
- (24) (a) Pichon, C.; Mialane, P.; Dolbecq, A.; Marrot, J.; Riviere, E.; Keita, B.; Nadjo, L.; Secheresse, F. *Inorg. Chem.* **2007**, 46, 5292. (b) Dias, V. L. N.; Fernandes, E. N.; da Silva, L. M. S.; Marques, E. P.; Zhang, J.; Marques, A. L. B. *J. Power Sources* **2005**, 142, 10. (c) Losada, J.; del Peso, I.; Beyer, L. *Inorg. Chim. Acta* **2001**, 321, 107.
- (25) (a) Solomon, E. I.; Ginsbach, J. W.; Heppner, D. E.; Kieber-Emmons, M. T.; Kjaergaard, C. H.; Smeets, P. J.; Tian, L.; Woertink, J.

- S. *Faraday Discuss.* **2011**, *148*, 11. (b) Solomon, E. I.; Sundaram, U. M.; Machonkin, T. E. *Chem. Rev.* **1996**, *96*, 2563.
- (26) Farver, O.; Pecht, I. In *Multi-Copper Oxidases*; Messerschmidt, A., Ed.; World Scientific: Singapore, 1997.
- (27) (a) Djoko, K. Y.; Chong, L. X.; Wedd, A. G.; Xiao, Z. *J. Am. Chem. Soc.* **2010**, *132*, 2005. (b) Kosman, D. *J. Biol. Inorg. Chem.* **2010**, *15*, 15.
- (28) (a) Tan, Y.; Deng, W.; Li, Y.; Huang, Z.; Meng, Y.; Xie, Q.; Ma, M.; Yao, S. *J. Phys. Chem. B* **2010**, *114*, 5016. (b) Farver, O.; Tepper, A. W. J. W.; Wherland, S.; Canters, G. W.; Pecht, I. *J. Am. Chem. Soc.* **2009**, *131*, 18226. (c) Thorseth, M. A.; Tornow, C. E.; Tse, E. C. M.; Gewirth, A. A. *Coord. Chem. Rev.* **2013**, *257*, 130.
- (29) (a) Fukuzumi, S. *Prog. Inorg. Chem.* **2009**, *56*, 49. (b) Fukuzumi, S. *Bull. Chem. Soc. Jpn.* **1997**, *70*, 1.
- (30) (a) Fukuzumi, S.; Ohkubo, K. *Coord. Chem. Rev.* **2010**, *254*, 372. (b) Fukuzumi, S. *Chem. Lett.* **2008**, *37*, 808.
- (31) (a) Fukuzumi, S.; Mochizuki, S.; Tanaka, T. *Inorg. Chem.* **1989**, *28*, 2459. (b) Fukuzumi, S.; Mochizuki, S.; Tanaka, T. *Inorg. Chem.* **1990**, *29*, 653. (c) Fukuzumi, S.; Mochizuki, S.; Tanaka, T. *J. Chem. Soc., Chem. Commun.* **1989**, 391.
- (32) (a) Fukuzumi, S.; Okamoto, K.; Gros, C. P.; Guillard, R. *J. Am. Chem. Soc.* **2004**, *126*, 10441. (b) Fukuzumi, S.; Okamoto, K.; Tokuda, Y.; Gros, C. P.; Guillard, R. *J. Am. Chem. Soc.* **2004**, *126*, 17059.
- (33) Halime, Z.; Kotani, H.; Li, Y.; Fukuzumi, S.; Karlin, K. D. *Proc. Natl. Acad. Sci. U.S.A.* **2011**, *108*, 13990.
- (34) (a) Peljo, P.; Murtomäki, L.; Kallio, T.; Xu, H.-J.; Meyer, M.; Gros, C. P.; Barbe, J.-M.; Girault, H. H.; Laasonen, K.; Kontturi, K. *J. Am. Chem. Soc.* **2012**, *134*, 5974. (b) Su, B.; Hatay, I.; Trojáněk, A.; Samec, Z.; Khoury, T.; Gros, C. P.; Barbe, J.-M.; Daina, A.; Carrupt, P.-A.; Girault, H. H. *J. Am. Chem. Soc.* **2010**, *132*, 2655. (c) Hatay, I.; Su, B.; Li, F.; Méndez, M. A.; Khoury, T.; Gros, C. P.; Barbe, J.-M.; Ersoz, M.; Samec, Z.; Girault, H. H. *J. Am. Chem. Soc.* **2009**, *131*, 13453.
- (35) (a) Devoille, A. M. J.; Love, J. B. *Dalton Trans.* **2012**, *41*, 65. (b) Askarizadeh, E.; Yaghoob, S. B.; Boghaei, D. M.; Slawinc, A. M. Z.; Love, J. B. *Chem. Commun.* **2010**, *46*, 710.
- (36) Fukuzumi, S.; Kotani, H.; Lucas, H. R.; Doi, K.; Suenobu, T.; Peterson, R. L.; Karlin, K. D. *J. Am. Chem. Soc.* **2010**, *132*, 6874.
- (37) Tahsini, L.; Kotani, H.; Lee, Y.-M.; Cho, J.; Nam, W.; Karlin, K. D.; Fukuzumi, S. *Chem.-Eur. J.* **2012**, *18*, 1084.
- (38) Fukuzumi, S.; Tahsini, L.; Lee, Y.-M.; Ohkubo, K.; Nam, W.; Karlin, K. D. *J. Am. Chem. Soc.* **2012**, *134*, 7025.
- (39) (a) Prins, R.; Kortbeek, A. G. T. G. *J. Organomet. Chem.* **1971**, *33*, C33. (b) Fukuzumi, S.; Chiba, M.; Ishikawa, M.; Ishikawa, K.; Tanaka, T. *J. Chem. Soc., Perkin Trans. 2* **1989**, 1417.
- (40) (a) Su, B.; Nia, R. P.; Li, F.; Hojeij, M.; Prudent, M.; Corminboeuf, C.; Samec, Z.; Girault, H. H. *Angew. Chem., Int. Ed.* **2008**, *47*, 4675. (b) Su, B.; Hatay, I.; Ge, P. Y.; Mendez, M.; Corminboeuf, C.; Samec, Z.; Ersoz, M.; Girault, H. H. *Chem. Commun.* **2010**, *46*, 2918.
- (41) The E_{ox} values of ferrocene derivatives in acetone are virtually the same as those in MeCN; see: Noviadri, I.; Brown, K. N.; Fleming, D. S.; Gulyas, P. T.; Lay, P. A.; Masters, A. F.; Phillips, L. *J. Phys. Chem. B* **1999**, *103*, 6713. Further, we checked to see if the E_{ox} values of ferrocene derivatives remain the same in the presence of $HClO_4$, and in fact they do (see Figure S7 in SI).
- (42) At higher temperature, however, $[Cu^{II}_2(XYLO)(OOH)]^{2+}$ started to decompose.
- (43) Sauer, M. C. V.; Edwards, J. O. *J. Phys. Chem.* **1971**, *75*, 3004.
- (44) Kunishita, A.; Scanlon, J. D.; Ishimaru, H.; Honda, K.; Ogura, T.; Suzuki, M.; Cramer, C. J.; Itoh, S. *Inorg. Chem.* **2008**, *47*, 8222.
- (45) Armarego, W. L. F.; Chai, C. L. L. *Purification of Laboratory Chemicals*, 6th ed.; Pergamon Press: Oxford, 2009.
- (46) Karlin, K. D.; Hayes, J. C.; Gultneh, Y.; Cruse, R. W.; McKown, J. W.; Hutchinson, J. P.; Zubieta, J. *J. Am. Chem. Soc.* **1984**, *106*, 2121.
- (47) Karlin, K. D.; Ghosh, P.; Cruse, R. W.; Farooq, A.; Gultneh, Y.; Jacobson, R. R.; Blackburn, N. J.; Strange, R. W.; Zubieta, J. *J. Am. Chem. Soc.* **1988**, *110*, 6769.
- (48) Mann, C. K.; Barnes, K. K. *Electrochemical Reactions in Nonaqueous Systems*; Marcel Dekker: New York, 1990.
- (49) (a) Mair, R. D.; Graupner, A. J. *Anal. Chem.* **1964**, *36*, 194. (b) Fukuzumi, S.; Kuroda, S.; Tanaka, T. *J. Am. Chem. Soc.* **1985**, *107*, 3020.